

PRESS-FIT ANALYSIS OF AXLE ASSEMBLY  
USING MSC/NASTRAN NONLINEAR CAPABILITY

by

H. N. Agrawal  
P. R. Perumalswami

Structural Analysis Department  
Advanced Vehicle Engineering and Technology  
Car Product Development  
Ford Motor Company  
Dearborn, Michigan 48121

Presented at the  
MSC/NASTRAN USER'S CONFERENCE  
Pasadena, California

March 22-23, 1984

Press-Fit Analysis of Axle Assembly Using  
Nonlinear Capability of MSC/NASTRAN

Abstract:

Experiences with NASTRAN material nonlinear capabilities applied to a practical finite element model are presented herein. A press-fit automotive assembly is analysed using MSC/NASTRAN MPC equations simulating the interference and the effects of material nonlinearities. Gap elements are introduced in order to study the effects of transverse forces which tend to loosen the joint. Also, some parameters of NASTRAN "NLPARM" card are studied in order to attain convergence.

Introduction:

Press-fit methods are widely used in automotive assembly operations because of simpler manufacturing and assembly tasks and to obtain desired joint strength for service loads. The basic press-fit analysis procedures are described in most of the text books on strength of materials which provide radial, tangential and axial stresses, strains and displacements for various interference fits and boundary conditions and external loads. The effects of transverse service loads on these assemblies, including separation of members at the joint, are not clearly established.

The axle which is analysed here consists of cast steel housing (trunnion) and swaged steel tube (tube) and is assembled by press-fitting and then slug-welding. The operation involves pushing the two tubes into a differential housing simultaneously until each tube penetrates about 4 inches. This assembly is subjected to service loads over and above the assembly loads and has to function as a unit without any separation or loss of lubricant.

A linear static analysis of the press-fit using highly idealized geometries showed stress levels exceeding the yield strength of the materials. In order to evaluate the assembly more realistically, at least a quarter of the axle cross-section and nearly full length axle model was desired. In this analysis, stress and deformation levels due to fully pressed-fit and the nonlinear material capability of MSC/NASTRAN are evaluated. Later, in order to evaluate the effects of transverse loads, the interference region is simulated by using NASTRAN GAP elements. Monitoring the gaps and displacements at various load factors, the stress and deformation values and the joint integrity are ascertained. In this process, various parameters of NASTRAN "NLPARM" card are also scrutinized in order to obtain convergence.

Model and Assumptions:

The axle assembly analyzed is as shown in Fig. 1. A quarter segment of the assembly with appropriate boundary conditions is considered to provide satisfactory results. A total of 432 HEXA solid elements and 840 grid points are used (Figs. 2 and 3). Full tube length and part of trunnion/housing length are modeled, assuming that the rest of the housing is relatively very stiff and does not involve plasticity since it is far away from the interference region. The following geometric and tolerance data in inches are used for this model.

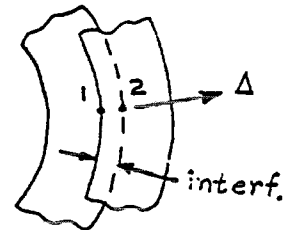
|          | Outside<br>Diam.  | Nominal<br>Diam. | Inside<br>Diam. | Thickness | Length | Interference |        |        |
|----------|-------------------|------------------|-----------------|-----------|--------|--------------|--------|--------|
|          |                   |                  |                 |           |        | length       | max.   | min.   |
| Tube     | 3.5025/<br>3.4975 | 3.5              | 2.54            | .480      | 27.0   | 4.0          | .00725 | .00275 |
| Trunnion | 3.492/<br>3.488   | 4.5              | 3.49            | .545      | 5.0    | 4.0          | .00725 | .00275 |

### Interference Modeling:

Consider points 1 and 2 lying at the interference on the tube and trunnion respectively; then radially

$$\Delta_{\text{interference}} = \Delta_1 - \Delta_2 = 100$$

$$\text{or } \Delta_1 - \Delta_2 - \Delta_{100} = 0$$



Assuming  $\Delta_2 > \Delta_1$ , then  $\Delta_{\text{intf.}}$  will be a negative quantity. Point 100 is very close to points 1 and 2.

A set of NASTRAN MPC equations in terms of cylindrical coordinate system are written to simulate the interference. Also sets of SPCD with .00725 inch value and SPC, FORCE cards with zero values are written in order to use NASTRAN effectively.

The stress-strain curves for materials involved are as shown in Figs. 4 and 5 and are defined using TABLES1 cards. The trunnion end is fixed to simulate the stiff housing connection. Von Mises yield function criteria (YF) and isotropic hardening rule (HR) are defined in MATS1 cards (although no unloading is involved in this case).

### Nonlinear Parameter Iteration Strategy:

A total of 6 load increments (LINC=6) with a maximum of 5 iterations for each load and tangent stiffness update method (KMETHOD) "SEMI" with convergence test (CONV) of "UPW" are used. All default tolerances are used for this strategy.

The solution converged after one iteration for each load up to a load factor of .5 due to linear material behavior and, therefore, no load error vector (/EPI/<10<sup>-11</sup>) was available to iterate on. However, starting from .667 load factor, it required 3 iterations for each load factor to converge. The convergence is achieved because of satisfying tolerances on UPW.

Results:

The load deflection curve for a typical point in the interference region is as shown in Fig. 6, which shows the material non-linearity starting at about .667 load factor. With the aid of "TIDE" (in-house) and "MOVIEBYU" post-processors, Von Mises stress levels, along with deformed shapes, are as shown in Appendix A. The trunnion is seen as moving inward as was expected. The end of the tube shows stress concentration above 60 KSI while the yield point from stress-strain curve (Fig. 4) is about 54.5 KSI, showing the plastic state of the tubing material. The trunnion having a yield of 41.2 KSI (Fig. 5) shows stress values of about 49 KSI toward the spindle end. The stress and deformation levels for a pair of typical points at the fit are as shown below:

|                  | <u>Elem.</u> | <u>GP</u> | <u>Radial</u> | <u>Tangential</u> | <u>Von Mises</u> | <u>Radial Disp.</u> |
|------------------|--------------|-----------|---------------|-------------------|------------------|---------------------|
| Tube             | 1085         | 1051      | -10536        | -41956            | 37691            | -.0031              |
| Trunnion         | 78           | 36        | -10426        | 47570             | 52435            | .00415              |
| Theory<br>Linear | Tube         | 1051      | -17054        | -55003            |                  | -.00253             |
| (Appendix B)     | Trunnion     | 56        | -17054        | 69282             |                  | .00406              |

The magnitude of axial stresses is small compared to radial and tangential stresses.

Gap Elements:

MPC equations are used in the previous analysis to strictly evaluate the effects of press-fit. To evaluate the effects of transverse loads on the axle, one has to model the press-fit to allow it to relax and even open at certain areas. MSC/NASTRAN gap elements are thought to provide such a capability for the model.

To understand the behavior of MSC/NASTRAN gap elements, a one-dimensional model of CELAS2 elements is used (Fig. 7).

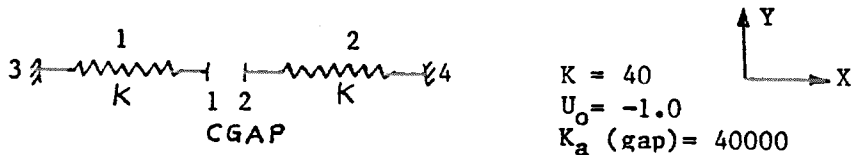


FIG. 7

Being a nonlinear element, SOL 24 disregarded the initial gap as was expected and worked as a linear spring. However, SOL 66 resulted in the following forces and displacements:

| GP | Disp.   | Elem. | Forces | Gap   |        |
|----|---------|-------|--------|-------|--------|
|    |         |       |        | Force | Disp.  |
| 1  | -.49975 | 1     | -19.99 | 19.99 | -.9995 |
| 2  | +.49975 | 2     | +19.99 |       |        |

"SEMI" method with 4 load steps and "UPW" criteria were used for convergence strategy. Full initial  $-1.0 (U_0)$  interference was applied and no other nonlinearities were involved; therefore, convergence was attained at each iteration.

To account for material nonlinearity along with the effects of the press fit, the method was extended to a model made of a slice of axle as shown in Fig. 8. A total of 30 HEXA are used for the outer tube and 72 HEXA for the inner tube. Eight gap elements are included at the interference region. Appropriate boundary conditions were again applied to simulate the symmetry of the model. Outer tube is fixed at the housing side.

A much smaller force ( $1.E-7$ ) was applied in the radial direction to execute NASTRAN. Elastic perfectly-plastic with 80 KSI and 49 KSI yield point materials were used for the inner and the outer tubes respectively on MATSI cards. An initial gap of  $-.00725$  in. for  $U_0$  and axial stiffness ( $K_a$ ) of  $1.+E8$  are used in PGAP card.

Parameters used in NLPARM cards were altered in order to obtain convergence. LINC, KMETHOD, MAXITER, CONV, EPSU were changed for different computer runs. Upon using "UPW" or "P" or "W" as the convergence criterion and "SEMI" or "AUTO" as the method of controlling tangent stiffness, the solution never converged and the rate of convergence ( $\lambda$ ) was very slow. The DLMAG ( $\|\delta^2\|$ ) was found to be small but EPI and EWI were very large due to very small applied force, as can be seen from the following expressions.

$$EPI = \frac{\|\delta^i\|}{\|P\|}$$

$$EWI = \frac{\{P + \delta^i\}^T \{u^i - u^{i-1}\}}{\{P\}^T \{u^i\}}$$

With "AUTO" -8 iterations and "U", the solution converged at second iteration for each load step. However, the first load step took 8 iterations to converge. DLMAG was of the order of  $10^{-4}$ ; however, EPI was of the order of  $10^6$ .

On changing the applied force from 1.-7 to .5 lb., the solution converged very swiftly and by the end of 4th load step U,P,W became of the order of 10<sup>-11</sup>. The following table summarizes the displacements and stresses for a pair of typical elements at press-fit region.

| Model  | NLPARM           | GP  | Stresses PSI |            |           | Disp.   | Gap Axial Disp. |
|--|------------------|-----|--------------|------------|-----------|---------|-----------------|
|  |                  |     | Radial       | Tangential | Von-Mises |         |                 |
| A MPC+M.N.<br>(no gaps)                          | SEMI,UPW<br>4-10 | 251 | -14384       | -43258     | 37557     | -.00226 | -               |
|  |                  | 503 | -11843       | 44313      | 49003     | .00499  |                 |
| B Gaps+M.N.                                      | AUTO,U<br>4-10   | 251 | 9589         | 34486      | 40813     | .00207  | -.00724         |
|  |                  | 503 | 14760        | -37860     | 49000     | -.00517 |                 |
| C Gaps+M.N.<br>+temper-<br>ature<br>(Appendix B) | AUTO,UPW<br>4-10 | 251 | 841          | 2624       | 2157      | .00817  | -.008           |
|  |                  | 503 | -.001        | +.004      | 0.        | 0.      |                 |

As can be seen from cases B and C (displacements and stresses), the inner tube is expanding outward while the outer is contracting inward. The gap elements are found to have interesting properties when they are used in the interference type of fit. The outer tube's inner surface was located inside the inner tube's outer surface as shown in Fig. 9. The equilibrium equation for the gap element is:

$$F_x - F_0 = K_a (U_a - U_b - U_0)$$

$-U_0$  = positive due to interference

$U_a - U_b$  = should be a negative number to transfer load.

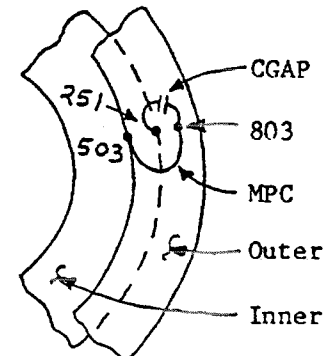


FIG. 9

In the cases described above,  $(U_a - U_b)$  was positive along with  $U_0$  and due to the nature of the definition of the model geometry. In order to circumvent this problem, new grid points outside of both interference surfaces were created (point 803 in Fig. 9) and gap elements were connected between the points of inner tube and these new points (251 to 803). Also, MPC equations connecting these new points and the points on the outer tube (803 to 503) were added to the model so that these points will stay together in all directions. Now the equation becomes

$$\begin{aligned} F_x &= K_a \{ U_{251} - U_{803} - (-.00725) \} \\ &= K_a \{ U_{151} - U_{803} + .00725 \} \end{aligned}$$

and ( $U_{251}-U_{803}$ ) will be a negative number due to geometric location of point 803. This method of interference fit simulation worked very well without compromising the model and results obtained were satisfactory and are summarized below.

| <u>Model</u>                                  | <u>NLPARM</u> | <u>GP</u> | <u>Stresses PSI</u> |                   |                  | <u>Disp.</u> | <u>Gap</u>         |
|---|---------------|-----------|---------------------|-------------------|------------------|--------------|--------------------|
|   |               |           | <u>Radial</u>       | <u>Tangential</u> | <u>Von-Mises</u> |              | <u>Axial Disp.</u> |
| A Gaps w/MPC<br>(No M.N.)                     | AUTO,U        | 251       | -14504              | -50176            | 52473            | -.00285      | -.00723            |
|   | 4-10          | 503       | -19198              | 67357             | 81317            | .00438       |                    |
| B Gaps w/MPC<br>+ M.N.                        | SEMION,U      | 251       | - 9286              | -32956            | 40731            | -.00204      | -.00724            |
|   | 4-10          | 503       | -11984              | 37107             | 49000            | .0052        |                    |
| C Theory, plane stress<br>linear (Appendix B) |               | 251       | -17054              | -55003            |                  | -.00253      |                    |
|   |               | 503       | -17054              | 69282             |                  | .00406       |                    |

Due to unsymmetrical nature of the transverse load and expected variations in the gap element openings/closings along the circumferential and longitudinal directions, a full model of the axle is needed. Upon availability of the full model, the press-fit will be analysed first by using  $U_0$  (in NASTRAN PGAP element) and, second, by applying temperature differential at outer and inner tubes.

#### Conclusions:

NASTRAN material nonlinear capabilities are successfully applied to a press-fit joint. The material nonlinearity along with nonlinear NASTRAN CGAP element effects are studied for the press-fit and the results are satisfactory.

Acknowledgements:

The authors wish to acknowledge

- the consulting help of Dr. R. Narayanswamy and MSC staff - Bob Harder, Dave Herting, Carl Hennrich, and Jerry Joseph;
- the initial contribution to this study by Mr. M. P. Zebrowski of Ford Motor Company;
- the funding support by Mr. B. K. Agrawal of Ford Motor Company;
- the encouragement of Ford Motor Company management at Structural Analysis Department - M. P. Anderson, V. J. Borowski, and W. B. Crum.

References:

1. T. V. Seshadri, "Effect of Transverse Forces on Shrink-Fit Assemblies", SAE paper 770611.
2. Harold A. Rothbart, "Mechanical Design and Systems Handbook", McGraw-Hill, 1964, pp. 23-1 to 23-12.
3. Jerrard A. Joseph, "MSC NASTRAN Application Manual", pp. 2.14-1 to 2.14-97, June 1983.

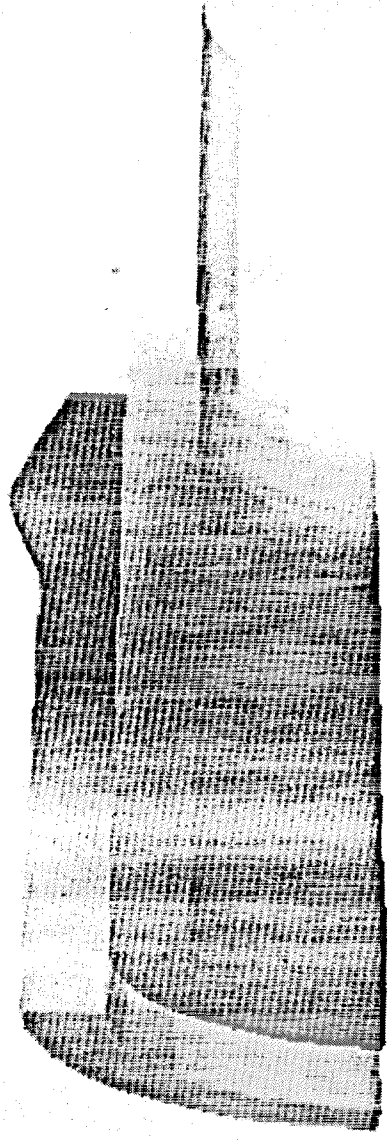


4.178-8 (13.1)

**Appendix A**

**Color Slides**

5000.000 15000.000 27000.000 38000.000 49000.000  
60000.000



SCALE NON LINEAR .00735 IN. INTERFERENCE  
VON MISES STRESS

Von Mises Stress Levels in lbs./sq. in.

## Appendix B

Stresses and displacements due to press fit (plane stress).  
 Diametral interference =  $(.00725 \times 2) = .0145 \text{ in.} = \Delta$

1. Radial stresses,
- $\sigma_r$

$$\sigma_r = \frac{E \Delta (d_c^2 - d_i^2) (d_o^2 - d_c^2)}{2 d_c^3 (d_o^2 - d_i^2)}$$

$$= 17054 \text{ Psi}$$

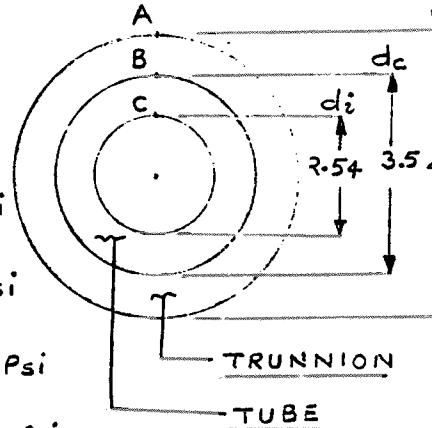
2. Tangential stresses,
- $\sigma_t$

$$\sigma_t \text{ (at A, trunnion)} = \frac{2 \sigma_r d_c^2}{d_o^2 - d_c^2} = 52228 \text{ Psi}$$

$$\sigma_t \text{ (at B, trunnion)} = \frac{\sigma_r (d_o^2 + d_c^2)}{(d_o^2 - d_c^2)} = 69282 \text{ Psi}$$

$$\sigma_t \text{ (at B, tube)} = \frac{-\sigma_r (d_c^2 + d_i^2)}{(d_c^2 - d_i^2)} = -55003 \text{ Psi}$$

$$\sigma_t \text{ (at C, tube)} = \frac{-\sigma_r (d_c^2)}{(d_c^2 - d_i^2)} = -72058 \text{ Psi}$$



3. Radial displacements (assume
- $\epsilon_z = 0$
- ),
- $\delta_r$

$$\Delta_r \text{ (at B, tube)} = \frac{(1+\nu)(1-2\nu)}{E} \times \frac{-\sigma_r d_c^2}{d_c^2 - d_i^2} \times \frac{d_c}{2} + \frac{1+\nu}{E} \times \frac{(-2\sigma_r)}{d_c} \times \frac{d_i^2 d_c^2}{4(d_c^2 - d_i^2)}$$

$$= -.002532 \text{ in.}$$

$$\Delta_r \text{ (at B, trunnion)} = \frac{(1+\nu)(1-2\nu)}{E} \times \frac{\sigma_r d_c^2}{d_o^2 - d_c^2} \times \frac{d_c}{2} + \frac{1+\nu}{E} \times \frac{(2\sigma_r)}{d_c} \times \frac{d_c^2 d_o^2}{4(d_o^2 - d_c^2)}$$

$$= .00406 \text{ in.}$$

4. Approximate temperature increment required to obtain diametral interference of .0145 is

$$(\Delta T) = \frac{\Delta}{\alpha d_c} = 637^\circ \text{ F}$$

Trunnion temperature  $70^\circ \text{ F}$

Tube temperature  $707^\circ \text{ F}$

Where  $\alpha$  = thermal coefficient of expansion  
 $\Delta$  = diametral interference  
 $E$  = modulus of elasticity  
 $\nu$  = Poisson's ratio

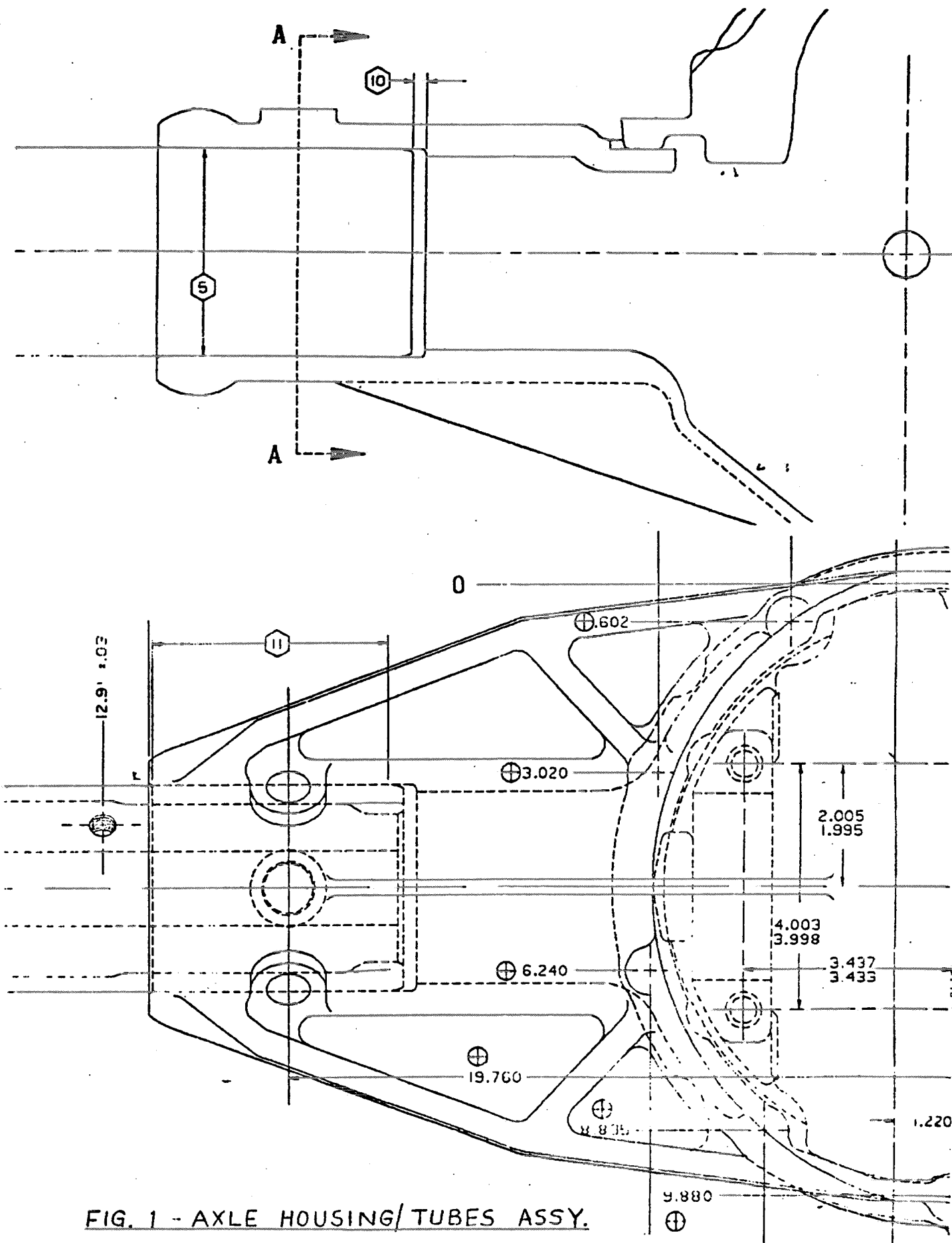


FIG. 1 - AXLE HOUSING/TUBES ASSY.

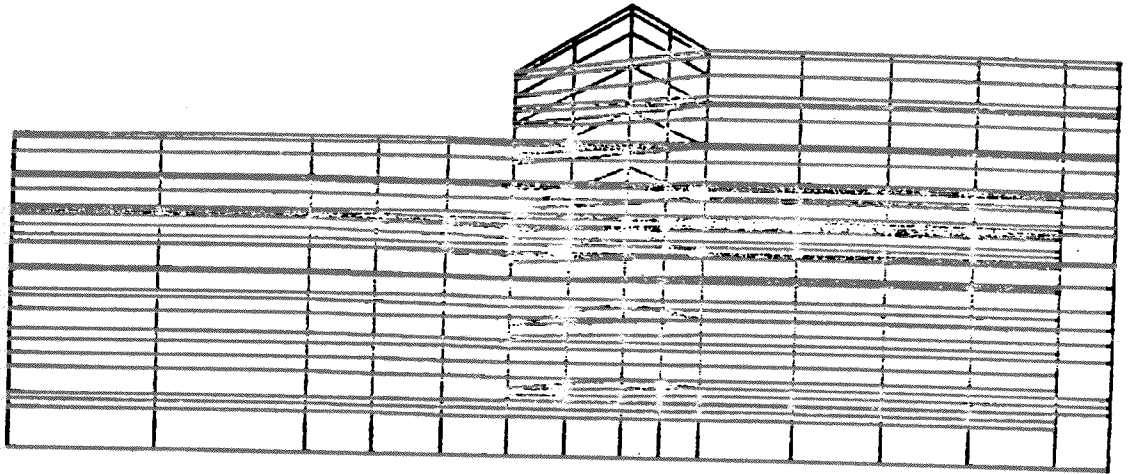


FIG. 2

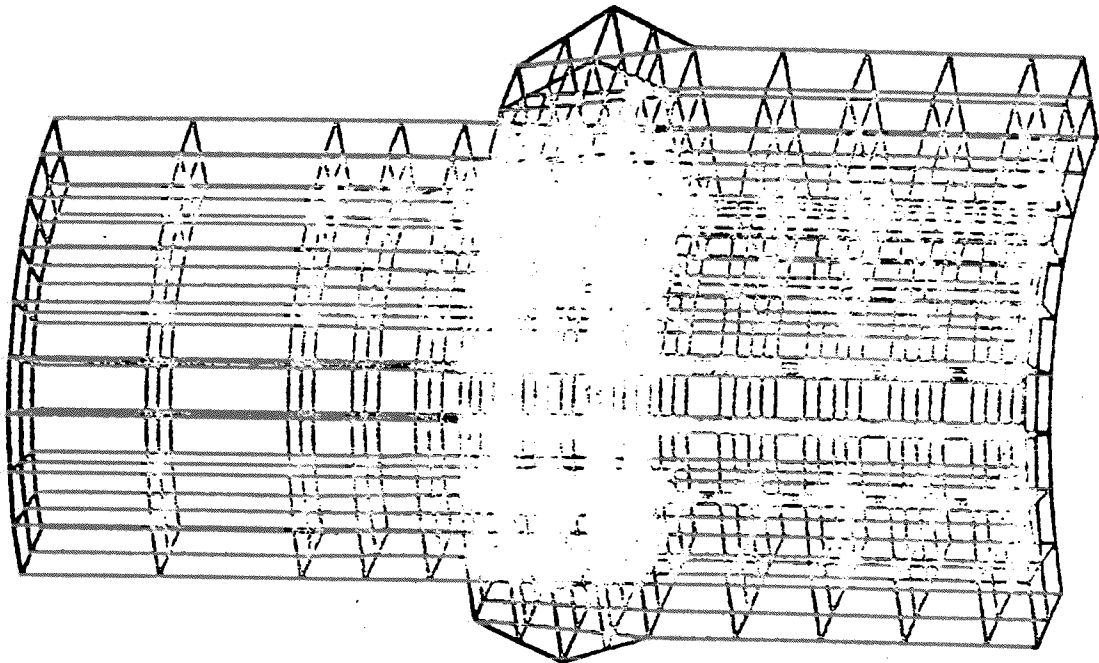
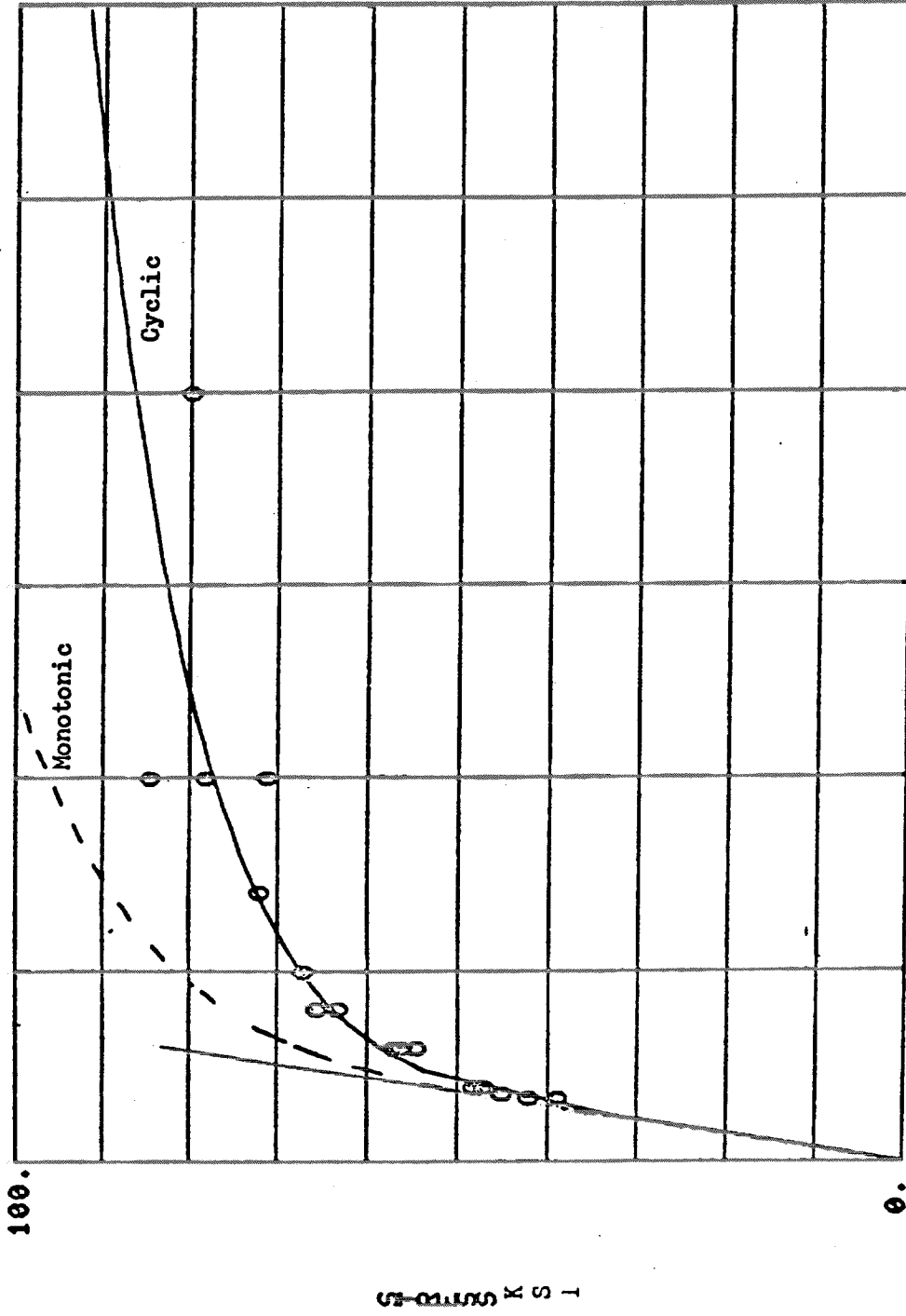


FIG. 3

SAE 1026 SWAGED



.03

STRAIN  
 KP = 148. NP = .132  
 KSI

FIG. 4 - TUBE MATERIAL STRESS-STRAIN CURVE

ASTM A536

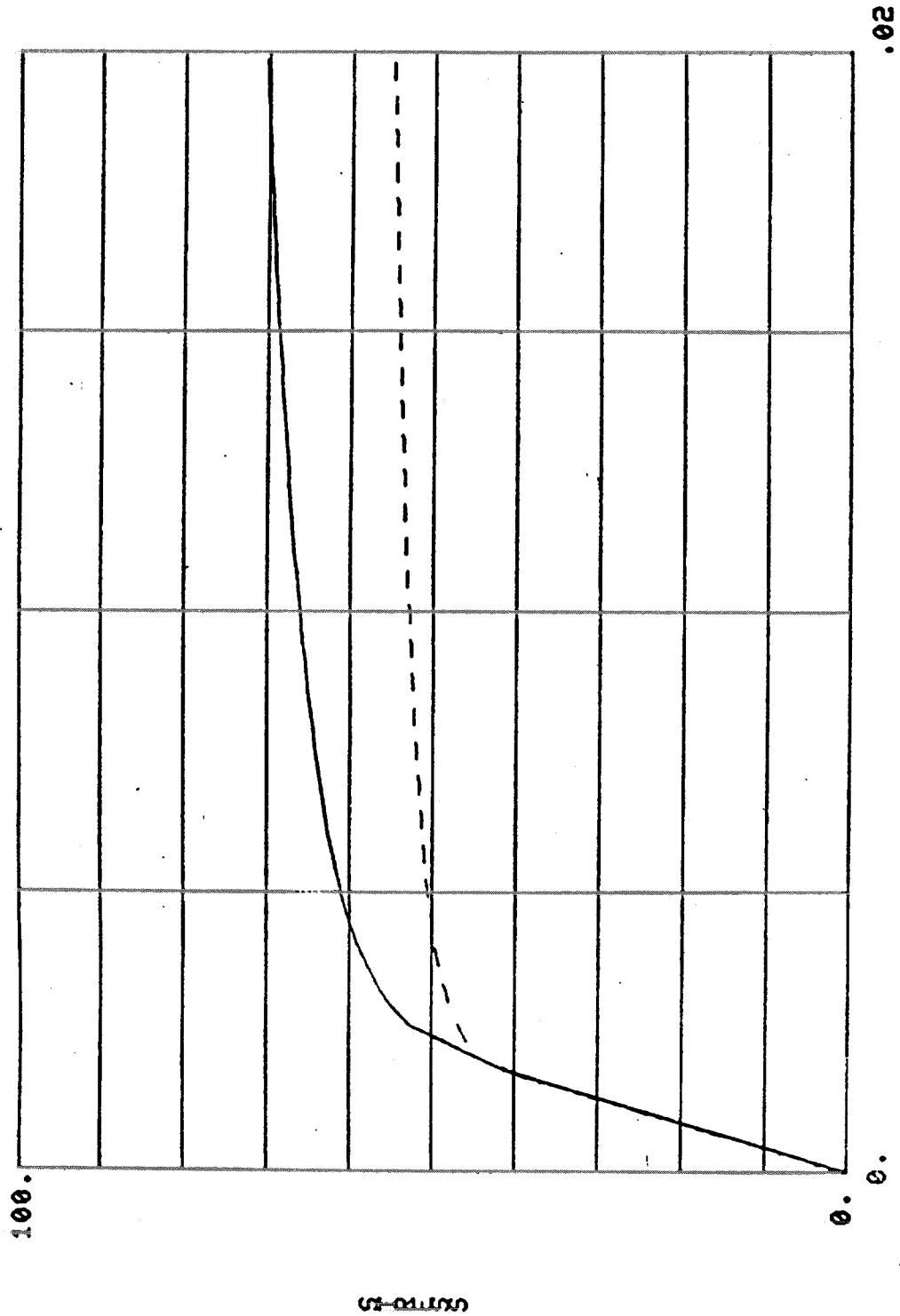


FIG. 5 - HOUSING MATERIAL STRESS-STRAIN CURVE

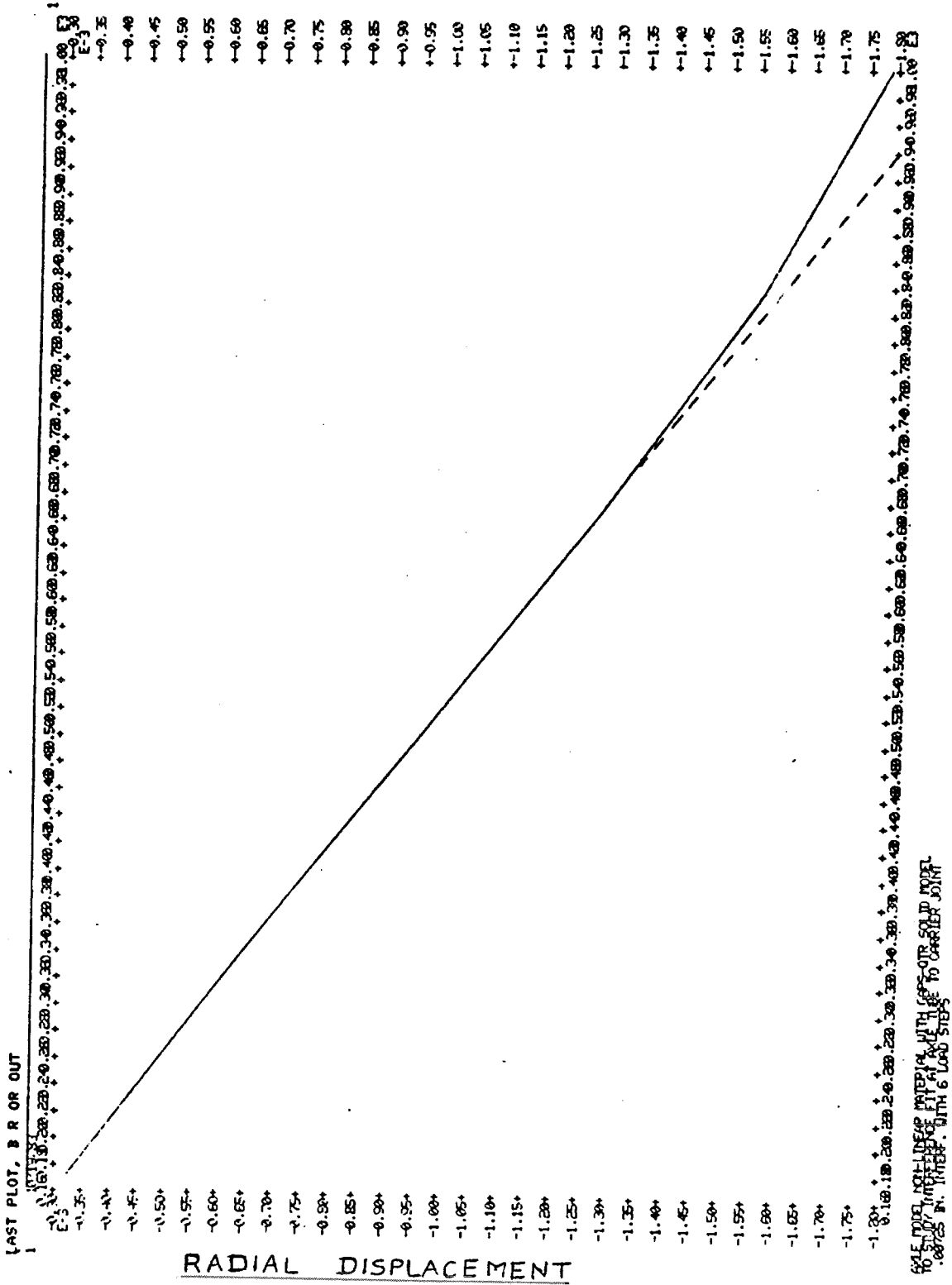
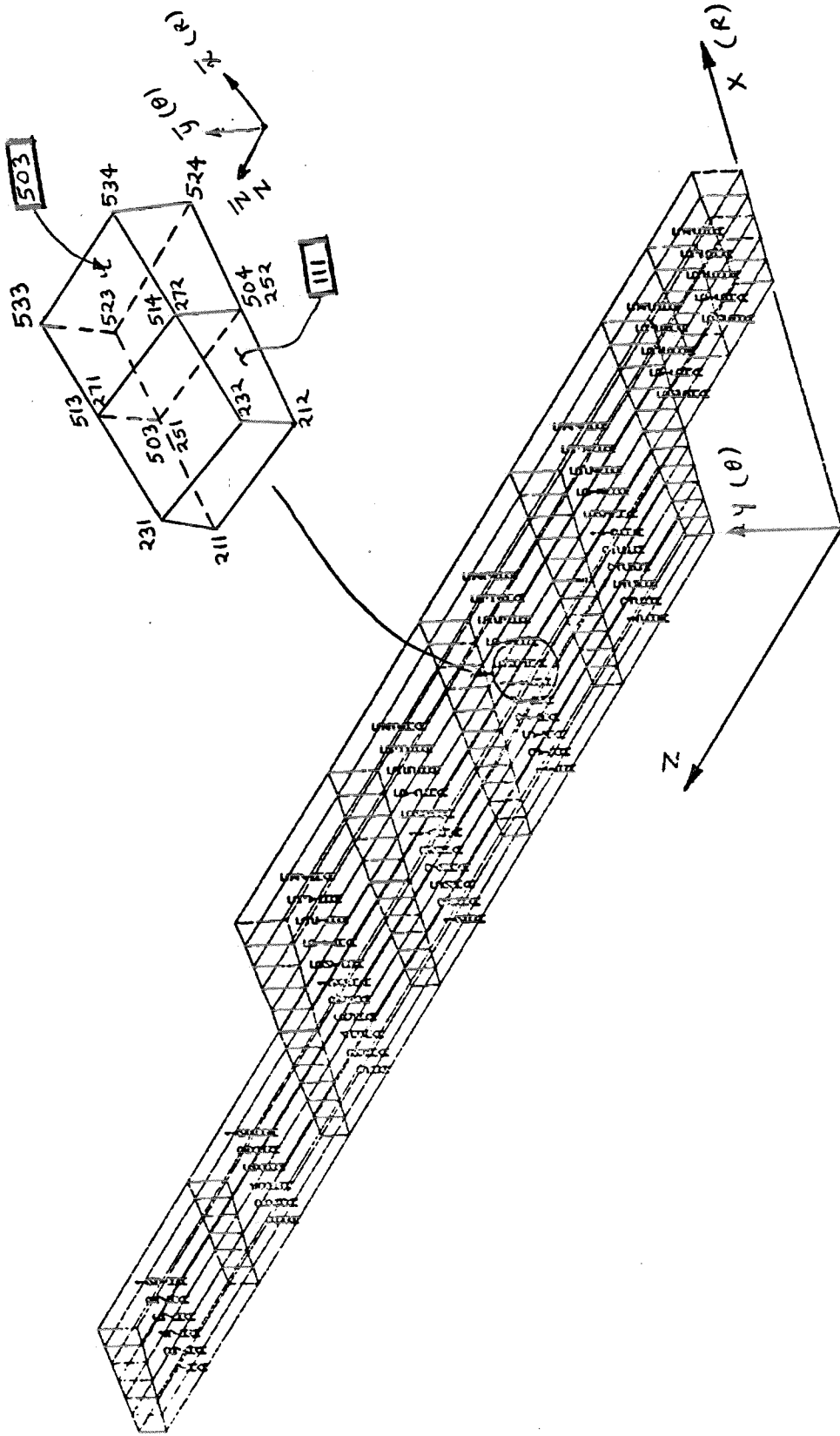


FIG. 6. LOAD-DEFLECTION CURVE FOR POINT 1075



HEXA EXAMPLE FOR ANGLE



HEXA EXAMPLE FOR ANGLE  
UNDEFORMED SHAPE

FIG. 8